

# IRIS RECOGNITION BASED ON LOCAL GREY EXTREMUM VALUES WITH CNN-BASED APPROACHES

Kamil Malinowski \* and Khalid Saeed 

*Faculty of Computer Science, Bialystok University of Technology, Bialystok, Poland*

*\*Corresponding author: Kamil Malinowski ([kamil.malinowski@sd.pb.edu.pl](mailto:kamil.malinowski@sd.pb.edu.pl))*

**Abstract** One of the most important steps in the operation of biometric systems based on iris recognition of the human eye is pattern comparison. However, the comparison of the recorded pattern with the pattern stored in the database of the biometric system cannot function properly without effective extraction of key features from the iris image. In the presented work, we propose an iris recognition system based on image feature extraction and extreme grey shade analysis. Harris-Laplace, RANSAC and SIFT descriptor algorithms were used to find and describe key points. In the experimental part, two methods were used to compare descriptors: the Brute Force method and the Siamese Network method. IIT Delhi Iris Database (version 1.0), MMU v2 database, UBIRIS v1, UBIRIS v2 image databases were used for the study. The proposed method utilizes a different approach when using the generalized corner extraction algorithm (Harris-Laplace algorithms) for comparing iris patterns. In addition, we prove that the use of the descriptor and the Siamese neural networks significantly improves the results obtained in the original method based on paths alone in the case of well contrasted infrared images with very low resolutions.

**Keywords:** biometrics, iris, grey extremum values, encoding.

## 1. Introduction

The iris is the opaque structure of the human eye. It is an element of the uveal membrane, located between the lens and the cornea. Its central element of variable diameter is called the pupil. Each iris has a pattern of discoloration, lining, and folds [1].

When looking for the optimal choice of a given biometric feature as an identification tool, many different factors should be considered. Each of the solutions used today has its strengths and weaknesses. One of the most important advantages of iris-based imaging systems is the statistically low rate of recognition errors. When making a choice, one should consider the adequacy of the solution to the satisfying needs related to identification. Nowadays, biometrics is the most important element in capturing systems. In addition, two-component systems, using biometrics and traditional solutions, are widely available and easy to use. An example may be the increasingly common biometric passports. It has become common to use biometrics in mobile devices, smartphones, tablets, laptops, where the standard is to install fingerprint readers and the iris of the eye. Biometrics is also becoming present in banking. More and more banks are working on the implementation of biometric systems as an effective identity control for customers, thus increasing the same level of security for their services. The iris pattern is very distinctive

and may not be sufficient to *uniquely* distinguish people. There are varieties of works that have already shown evidence of aging of the iris pattern [2].

Identity verification solutions based on biometric methods are used to control access to resources, also fulfilling the role of blocking unauthorized access attempts.

There are various neural network architectures that have been used for iris pattern recognition. Each of them has drawbacks that are worth discussing.

One of the main challenges of UniNet [3] is its accuracy, which largely depends on the quality of the data entered into it. A study by Zao et al. [3] shows that the accuracy of the UniNet algorithm in iris recognition is about 98.4%, so there is still room for improvement. Another disadvantage of this technology is the need for proper lighting and positioning of the eye, which can be difficult in some situations, such as performing identification at long distances or in low light, as discussed in the work of Hajari et al. [4].

The disadvantage of DRFNet [5] and GraphNet [6] is that they require a large amount of training data, which can be difficult to obtain. In addition, their implementation can require significant computing power.

Iris recognition using Siamese neural networks and point descriptors is one of the modern approaches in the iris recognition problem. The idea behind the creation of Siamese neural networks was to develop a method for comparing similarities for very complex data samples. The advantage of this method is the ability to compare data samples that have different characteristics and types. A well-constructed Siamese network is able to indicate subtle differences between two seemingly identical data samples [7].

When combined with point descriptors such as SIFT (Scale-Invariant Feature Transform), SURF (Speeded Up Robust Features), ORB (Oriented Fast and Rotated BRIEF) [8,9,10,11], Siamese networks can create a highly accurate iris recognition system. The point descriptors are responsible for detecting characteristic points on the image and generating vectors describing these points. One advantage of this approach is that point descriptors can be used to recognize the iris, even if it is not fully visible in the image. Additionally, Siamese networks with point descriptors have the ability to generalize and can operate with high efficiency on training and test data from different sources [8,9,10,11].

A novel method for image matching using extreme grey shade values and the SIFT descriptor was described in a publication by Zhao et al. [10]. The method is based on the use of extreme grey shade values of the image, which have unique characteristics. The authors proposed using the SIFT descriptor to extract characteristic points on the image and create vectors describing these points. Then, the selected extreme grey shade values are also added to the feature vector. The next step is to use a classification algorithm that can learn to recognize image based on the created feature vectors. The results of the authors' experiments show that the proposed method achieves an efficiency of 99.33% in image recognition. It is worth noting that despite the promising results, the method requires further research and testing on larger data sets to confirm its effectiveness and applicability in real applications.

Iris recognition systems can be vulnerable to fraud attempts, such as trying to present artificially generated iris images. Research focused on increasing resilience to such types of fraud is crucial for enhancing system security. The diversity of methods for comparing iris patterns makes such fraud attempts challenging. The aim of our study was to develop a new method for verifying individuals based on the iris by using properly extracted key points with associated descriptors, which could serve as another alternative to existing methods. Can a method using descriptors of points extracted from paths of extreme value for greyscale be effective in solving the problem of comparing iris patterns? We made a significant improvement to the original algorithm in [12]. Our modification involved extracting key points and analysing the SIFT descriptors of these points using Siamese neural networks. As a result, the algorithm has become resistant to various lighting conditions and changes in the position of the registered object. Information about the iris structure and its characteristics can be extracted from the paths of extreme values for shades of grey, which can be an extension of the methods previously described and can significantly improve their efficiency. The merit of descriptors combined with appropriate extraction of key points is to enhance the features and increase the diversity of iris patterns. The authors noted the great potential and effectiveness of comparing patterns using a technique based on comparing outlier paths based on shades of grey. Unlike the original method, ours proved more efficient for more than one set of irises. The original extracting extreme value paths approach used in proposed method is discussed in detail in Section 3.

## 2. State of the art

Nowadays, iris extraction is becoming more efficient and accurate thanks to developing technologies. With the increasing number of available iris databases and developing extraction algorithms, it is possible to achieve very high accuracy in iris recognition. One of the most important developments in the field of iris extraction is the introduction of methods using artificial neural networks. Neural networks make it possible to recognize irises more accurately and quickly, which contributes to the efficiency of this method.

However, it is worth remembering that iris extraction is still a process that requires high precision and accuracy. Many factors must be taken into account, such as image quality, distance from the camera and the health of the eye, in order to obtain accurate results. Therefore, research is still being conducted to develop more efficient iris extraction methods and to improve the quality of data sets.

The current trend in research on comparing iris patterns is the use of CNN (Convolutional Neural Network). A disadvantage of using CNN is its sensitivity to the quality of training data. Researchers use artificial neural networks in various ways to solve the problem of iris recognition. Lee et al. [13] used three CNN (Convolutional Neural Network) models for extracting features from images of the iris. The developed model uses

a non-square filter, and each CNN model is composed of eight convolutional layers and three fully connected layers. In this method, two additional regions are extracted – iris and periorbital region containing information about the shape of eyelids, eyebrows, and skin colour. From these regions and blurred and normalized iris, feature vectors are extracted and compared using SVM (Support Vector Machine). The proposed solution is sensitive to eyelid shape change, light reflection noise, and eyelashes. Yang et al. [14] pre-trained ResNet-18 model was used as an encoder of the created system – as an encoder skeleton for extraction of multi-level features. High-level functions have made it possible to capture more contextual information. The low-and high-level functions are combined by the Spatial Awareness Function Combine (SAFFM) module. Minimum Shifted and Masked Distance (MMSD) is used to compare the encoded irises. The authors achieved the Equal Error Rate (EER) factor of 0.27% for the developed method. Chen et al [15] used proposed method called NSNet (convolutional neural network based on the attention mechanism). Raw image without iris extraction was taken as input for feature extraction and recognition. The average EER (Equal Error Rate) factor is 0.343%. Winston et al. [16] tried to solve the problem of limited availability of data sets, which has a direct impact on the accuracy of classifiers. They have empirically proved that Adam based optimization is good at learning iris features using deep learning. According to the conducted research, the hybrid network of deep learning with SVM is the most appropriate method of recognizing the patterns of the iris of the eye, reaching the accuracy of 97.8%. Liu et al. [17] using image blur with three filters increased the accuracy of the methods of recognizing iris patterns using deep learning techniques. Chen et al. [18] is another work that uses CNN to compare the irises of the eye. The proposed method used a novel loss function called T-Center loss to enhance the discriminant ability of deep models. To avoid the gradient explosions and identify the appropriate hyperparameter, their approach simultaneously normalizes the feature vectors and feature center vectors. Despite the sensitivity of fuzzy, mirror reflections and reflections confirmed by the authors, the method gave satisfactory results. Liu et al. [19] 2-channel CNNs were used to recognize the iris. In the 2-channel CNN, the authors introduced four key innovations, including a large-scale hybrid iris identification and verification framework, a radial attention layer for weighing different regions of the iris, online expansion schemes to increase resilience, and structural reduction to lower computational load to improve performance. Ahmadi et al. [20] proposed a method based on two-dimensional Gabor kernel (2-DGK), polynomial filtering, and step filtering to solve the problem of iris recognition. The accuracy of the method is 95.36%. The same authors tried to improve their work and hence in [21], they proposed an algorithm using “hybrid radial basis function neural network (RBFNN) with genetic algorithm (GA) for matching task” and obtained an accuracy of 99.99%, but this time the procedure took much time (860.70 s).

Classic methods of iris pattern recognition have several advantages compared to those

using CNN. One of them is the requirement of incomparably fewer computational resources and memory. They are also simpler to understand and implement independently. Wang et al. [22] used an improved algorithm, based on wavelet packet transformation, to improve the iris recognition. The article uses the db4 wavelet base and Shannon entropy to decompose a normalized iris image. The iris recognition system uses Hamming distances. The authors declare the recognition effectiveness of the developed method at 96.3%. Bala et al. [23] the authors managed to improve the method based on the Xor-Sum Code (IXSC), allowing it to be used to recognize the iris both in the visible and infrared light. The EER ratio is at the level of 8.27%. Galdi et al. [24] proposed a multi-classifier based on three descriptors: colour, texture, and clusters. The method achieved an EER of 0.29. The authors have released the source code of the method they developed. This made it possible to compare the results obtained by us. Lv et al. [25] in their method used an odd symmetric 2D Log-Gabor filter to analyse the phase and amplitude of the iris texture in relation to different frequencies and orientations, and use feature fusion to eliminate noise. Abbasi et al. [26] using a binary genetic algorithm, they choose the best combination of various wavelet transforms, Fourier transforms, and Gabor filter. The proposed method has achieved a FAR (False Acceptance Rate), of 0 and a FRR (False Rejection Rate) of 0.092. Barpanda et al. [27] to extract iris features in their method they use wavelets from the Cohen-Daubechies-Feauveau 9/7 filter bank. This method has been improved [28] by using the Mel-frequency cepstral coefficients (MFCCs) to differentiate iris tissues. Gad et al. [29] segment the iris using the Delta-Mean (DM) method proposed by them. At the stage of extracting the features of the iris, an algorithm is used that combines the frequency and location of the features – multi-algorithm mean. The average accuracy of the algorithm is 99.48% while EER is 0.28. Yao et al. [30] using Harr and log-Gabor transforms, they achieved a recognition accuracy of 95%.

### 3. Proposed method

The goal of our research was to create a new method for comparing human iris patterns using known and publicly available algorithms. The algorithm should detect subtle differences in data samples, which would allow it to more precisely and effectively recognize iris patterns recorded in various environments. We proposed to use the Harris-Laplace, RANSAC (Random Sample Consensus) and SIFT descriptor algorithms to find and describe key points in the iris. The extracted key points of the studied iris are compared to those in the database using two Brute Force methods and Siamese neural networks. The proposed method is unique and easy to implement. For the sake of our goal, we used three iris bases in our research, namely IIT Delhi Iris Database (Version 1.0) [31], MMU.v2 database [32], UBIRIS v1 [33]. Since the iris images in the aforementioned databases were recorded in a restricted environment, we chose the UBIRIS v2 database [34] to

compare the performance of proposed method in an unrestricted environment. In the above-mentioned collection of the irises of the eye, the outer and inner boundaries are not always a perfect circle, which is directly related to the angle at which the image was recorded. Therefore, the assumption that the center of the pupil of the eye is located in the center of the captured image may be a mistake. For the initial determination of the pupil area, we used the diagrams developed in our previous articles [35,36]. Images from UBIRIS v1 [33] have been converted to greyscale. Proposed method does not take into account iris rotation. Unfortunately, in the case of the UBIRIS v2 database [34], classical iris segmentation algorithms such as the one developed by us are not effective enough for the proposed iris pattern recognition method to work properly. For this database, we used the method developed by Omar et al. [37]. For the other bases, we describe below the iris extraction method we developed in previous articles.

The boundaries of the iris in images recorded at an angle other than a right angle are shaped like an ellipse. To eliminate image distortion and convert the elliptical boundaries of the iris into a circle in the area of the pupil, a rectangle is circumscribed. Having information about three points lying at the vertices of the rectangle  $(i'_1, j'_1)$ ,  $(i'_2, j'_2)$ ,  $(i'_3, j'_3)$ , we are able to find the affine transformation of this object into a square:

$$\begin{aligned} (i_1, j_1) &\rightarrow (i'_1, j'_1), \\ (i_2, j_2) &\rightarrow (i'_2, j'_2), \\ (i_3, j_3) &\rightarrow (i'_3, j'_3). \end{aligned} \tag{1}$$

For the points belonging to the vertices of the square  $(i_1, j_1)$ ,  $(i_2, j_2)$ ,  $(i_3, j_3)$ , one should find the transformation coefficients  $(a_{00}, a_{01}, a_{02}, a_{10}, a_{11}, a_{12})$  by solving the system of equations (2):

$$\begin{bmatrix} i_1 \\ j_1 \\ i_2 \\ j_2 \\ i_3 \\ j_3 \end{bmatrix} = \begin{bmatrix} i'_1 & j'_1 & 1 & 0 & 0 & 0 \\ 0 & 0 & 0 & i'_1 & j'_1 & 1 \\ i'_2 & j'_2 & 1 & 0 & 0 & 0 \\ 0 & 0 & 0 & i'_2 & j'_2 & 1 \\ i'_3 & j'_3 & 1 & 0 & 0 & 0 \\ 0 & 0 & 0 & i'_3 & j'_3 & 1 \end{bmatrix} \begin{bmatrix} a_{00} \\ a_{01} \\ a_{02} \\ a_{10} \\ a_{11} \\ a_{12} \end{bmatrix}. \tag{2}$$

In such a transformed image, determining the pupil center  $(x_0, y_0)$  inscribed in the square becomes a trivial task. The next stage of isolating the iris of the eye is to identify two points  $(x_1, y_1)(x_2, y_2)$  lying on the outer border of the iris [34]. From the indicated points and the pupil center, the radius of the circle is determined, to which these points belong:

$$R = \frac{\sqrt{(y_1 - y_2)^2 + (x_1 - x_2)^2} * \sin\left(\frac{\pi}{2} - \tan^{-1}\left|\frac{y_1 - y_2}{x_1 - x_2}\right|\right)}{\sin\left(\pi - 2\left(\frac{\pi}{2} - \tan^{-1}\left|\frac{y_1 - y_2}{x_1 - x_2}\right|\right)\right)}. \tag{3}$$

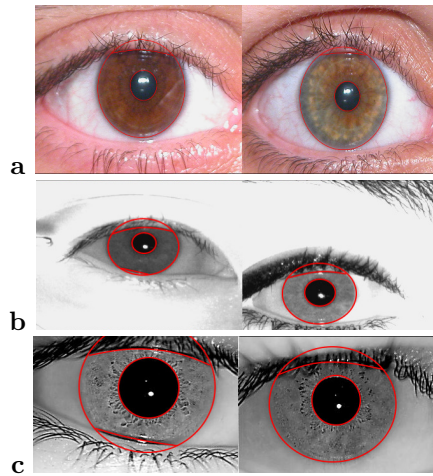


Fig. 1. Iris segmentation – (a) UBIRIS v1 [33], (b) MMU.v2 database [32], (c) IIT Delhi Iris Database (Version 1.0) [31].

The result of determining the boundaries of the outer and inner iris of the eye is shown in Fig. 1.

Iris normalization is aimed at transforming the area of the iris separated at an earlier stage into an area of constant size, regardless of the previously separated area of the iris. Obtaining consistent sizes is essential for the iris comparison procedure. Normalization ensures resistance to discrepancies in the size of the irises caused by the dilating pupil – resulting from different environmental conditions in which the image was recorded. All of images have been reduced to the size of  $240 \times 340$  pixels.

In this work, the conversion of the Cartesian coordinates  $(x, y)$  to coordinates in the non-concentric polar system  $(p, \theta)$  was used:

$$\begin{aligned} p &= \log \sqrt{(x - x_c)^2 + (y - y_c)^2}, \\ \theta &= \text{atan2}(y - y_c, x - x_c), \end{aligned} \quad (4)$$

where  $(x_c, y_c)$  – pupil center coordinates.

The result of applying the mathematical transformation to the iris image is an image with a constant size of  $240 \times 60$  pixels (Fig. 2). To enhance texture details of the iris, we used adaptive histogram equalization (CLAHE).

Proposed algorithm is based on changes in the intensity of points in stripes of constant size. As in the work of Rathgeb et al. [12], point intensity paths are extracted.

The pre-processed iris image  $I$  is divided into 15 stripes with a width of 4 points

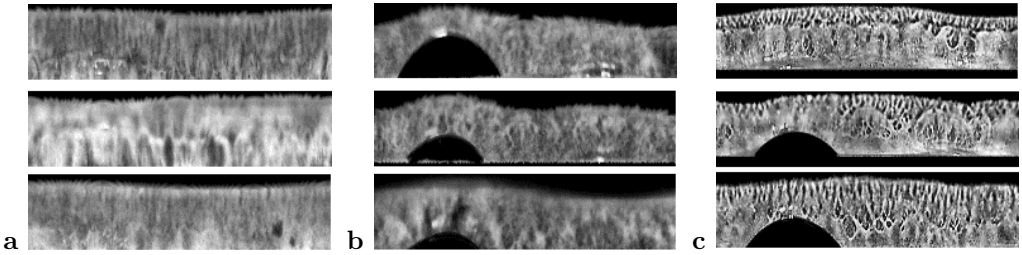


Fig. 2. Modified iris image of the eye – (a) UBIRIS v1 [33], (b) MMU.v2 database [32], (c) IIT Delhi Iris Database (Version 1.0) [31].

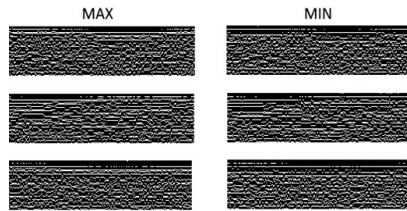


Fig. 3. Examples of extraction of paths of the variability of point values – maximum, minimum.

according to the formula (5) as in the work of Rathgeb et al. [12]:

$$I \rightarrow \{I_1, I_2, \dots, I_{15}\}. \tag{5}$$

From each iris image of the eye, 15 paths are extracted for points with maximum and minimum values in each of the strips  $P_L$  and  $P_H$  (6).

$$P_L = \left\{ \begin{matrix} P_{L1} \\ P_{L2} \\ P_{L3} \\ \dots \\ P_{L15} \end{matrix} \right\}, \quad P_H = \left\{ \begin{matrix} P_{H1} \\ P_{H2} \\ P_{H3} \\ \dots \\ P_{H15} \end{matrix} \right\}. \tag{6}$$

The detected paths are shown in Figure 3. Black marker without texture corresponds to the area covered by eyelashes, eyelids – these are areas of complete blackness or areas of white colour.

In the described method, points extracted from the paths of maximum and minimum values from the iris image are analysed. The path is formed by the local extremes of grey shade values, excluding the maximum – white colour and minimum – black colour. Thus, the analysis is carried out in relation to the extremes of grey shades. Selected conventional techniques support the process of minimizing the elements to be analysed,

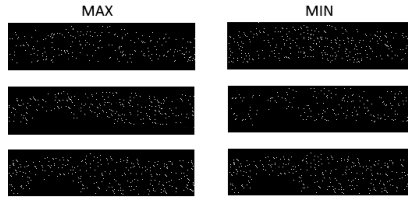


Fig. 4. Examples of key point extraction prior to RANSAC application.

making the process more efficient and comparable in effectiveness to the other techniques discussed in the manuscript.

Proposed method is based on the search for key points in the images shown in Fig. 3. Classic feature extraction methods by means of a key point detector use a region descriptor around each of the detected points. The main purpose of the descriptors is to isolate the characteristics of the information near each key point. Based on previous studies [38, 39], experiments were carried out to select the best feature descriptor from among the descriptors (SIFT – Scale-Invariant Feature Transform, Principal Component Analysis PCA-SIFT, GLOH – Gradient Location and Orientation Histogram, SURF – Speeded Up Robust Features).

In this study, we used a method based on Harris-Laplace [40] (7) and SIFT keypoint descriptor [41] algorithms. The features obtained using SIFT are constant in scale and rotation of the image. The SIFT descriptor creates a vector of the values of the orientation histogram in the region of each key point. These quantities are determined by the gradient and the orientation around the key points. The use of Laplacian-of-Gaussian makes the detected points resistant to changes of scale  $\sigma_1$  and can be detected in the image after resizing it. The combination of the above algorithms ensures repeatability of features and scale invariant fit.

$$R = g(I_x^2)g(I_y^2) - [g(I_x I_y)]^2 - \alpha [g(I_x^2) + g(I_y^2)]^2, \quad (7)$$

where  $\alpha$  was experimentally set at 0.42. Meanwhile,  $R$  values greater than 4.8 indicate a detected corner.  $I_x$  and  $I_y$  are the respective derivatives in the  $x$  and  $y$  direction applied to the smoothed image and calculated using a Laplacian-of-Gaussian (LoG) filter  $g$  with scale  $\sigma_D = 8\sigma_1$ . The  $\sigma_1$  parameter determines the current scale at which the Harris corner points are detected.

Only the key points in the images of the extracted paths are subjected to further analysis. Figure 4 shows the key points for each path.

The feature matching process is to find matching points on the recorded image and the pattern in the database. Once the points and their descriptors have been extracted, the goal is to find consistent matches across all the iris images. We introduced location restrictions [39]. Applying localization constraints reduces the time needed to process

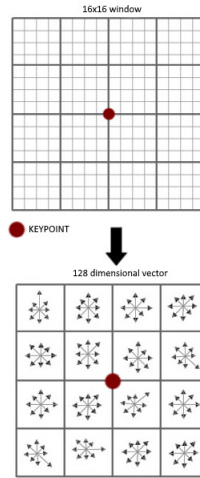


Fig. 5. Localization of a key-point.

the descriptors and prevents false matches. The iris area has been divided into four sections (Fig. 8). The point descriptors are in the same areas regardless of possible scale differences. We used the RANSAC algorithm to eliminate points with erroneous features. Experimentally and through the analysis of research on descriptor comparison methods [42], we decided to use the Brute Force method.

In the Brute Force method, the descriptors from all features must be matched to the descriptors of all features in another image. This is an extremely time-consuming solution. The method guarantees obtaining a solution without any guarantee that the solution is optimal. The Brute Force method uses the Euclidean distance between two descriptors. A smaller distance  $d_v$  indicates greater similarity between two points (8).

$$d_v(v_1, v_2) = \sqrt{\sum (v_1 - v_2)^2}, \tag{8}$$

where  $v_1, v_2$  – two feature description, SIFT feature descriptor will be a vector of 128 elements (16 blocks  $\times$  8 values from each block – Figures 5-6).

Although previous studies have shown that feature extraction methods are resistant to cluttered images [40], we decided to remove areas of the iris obscured by the eyelids using a method developed by us [36]. This procedure allows us to increase the quality of detected key points. Figure 7 shows a block diagram of the method we propose.

The percentage of similarity  $P$  between two images can be calculated using formula (9):

$$P = |CF|/|TF|, \tag{9}$$

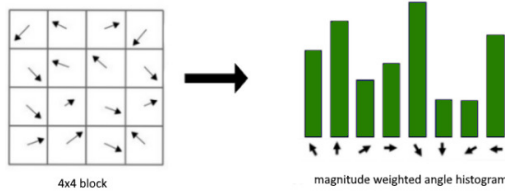


Fig. 6. Structure of a single block 4 × 4.

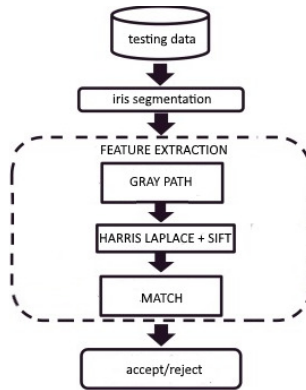


Fig. 7. A block diagram of the proposed method.

where CF is the correctly matched features after applying the RANSAC algorithm, TF is the total number of matches. A  $P$  value closer to 1 indicates a high degree of similarity between the analysed irises.

The problem of correctly matching the iris pattern to the correct person can be generalized to the multiclassification problem known from deep learning methods. Considering the drawbacks of the Brute Force method, we decided to use the Siamese Network [43] for iris pattern classification. The structure of a Siamese network can be compared to two other neural networks working side by side. Both networks have the same structure



Fig. 8. Division of key points into four areas of equal width after applying RANSAC.

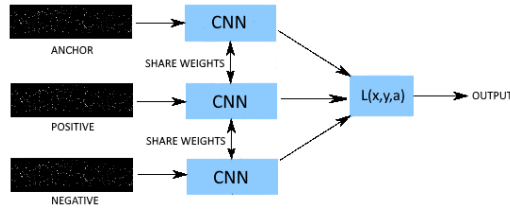


Fig. 9. Siamese Network structure used to compare SIFT descriptors.

and the same weights. These networks are then combined using a function that calculates a measure of similarity or distance. The structure of our Siamese network is shown in Figure 9.

The Siamese Network output aims to measure the similarity between two feature vectors obtained from CNNs. We were guided by the hypothesis that descriptors describing extracted points of the same iris will have similar feature vectors, which is equivalent to a small distance between them. Similarity between feature vectors can be measured using multiple distance metrics. During the training phase of the convolutional Siamese Network, we used the Triplet Loss Function:

$$L(x, y, a) = \max(0, d(a, x) - d(a, y) + m), \quad (10)$$

where two iris descriptor vectors of the same person and an iris descriptor vector of another person are selected randomly. The vectors of iris descriptors belonging to the same person are considered similar, so one is used as an anchor  $a$  and the other as a positive  $x$ , while the vector of iris descriptors of another person is considered negative,  $m$  is a margin value to keep negative samples far apart. In this paper, we used the CNN network architecture proposed in [44] shown in Fig. 10. The neural network architecture was chosen because of the high similarity of our input signal to the one used in the aforementioned work. The magnitude weighted angle histogram obtained from each point can be written in the form of a one-dimensional vector, which in turn is a kind of equivalent of recording the signal path – wave (Fig. 11). The input vector is created by starting from the point closest to the upper-left corner of the image, and then adding points located on the same path towards the right edge. This process is applied to each path.

#### 4. Experimental result

The aim of the experiments was to achieve accurate iris pattern classification results using descriptors of points extracted from paths of extreme value for greyscale. The selection of the similarity value is crucial for the correct decision to confirm or reject

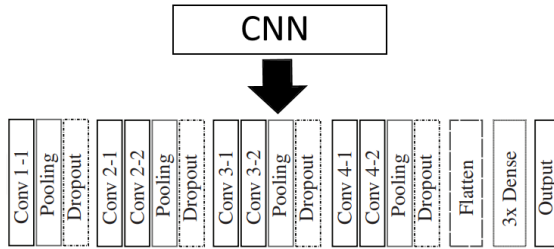


Fig. 10. Diagram of a single CNN network structure.

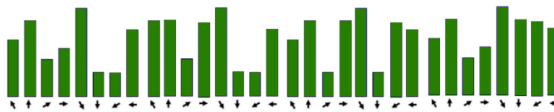


Fig. 11. Graph of SIFT descriptors points as a one-dimensional vector.

the user’s identity. The estimated similarity threshold separating the two results of the biometric verification has been considered. The verification result may or may not match the pattern.

Determining the optimal value for the similarity threshold required image analysis for two types of collections of the iris of the eye. The trials were made on the irises of the same people (mated-comparison) and on the irises of different people (non-mated comparison). Images of the left and right eyes of the same person were treated as if they belonged to two different people. The value of the similarity  $P$  threshold of which the images of irises are considered to be from the same person was experimentally set at 0.38. Data from all the databases were used to determine the  $P$  threshold. The choice of the  $P$  threshold is illustrated by the graph shown in Fig. 12.

For experimental purposes, we made our own implementation of the algorithms: Wang et al. [22], Yao et al. [30], Rathgeb et al. [12]. All these algorithms were tested under the same experimental conditions.

We first analysed the method using the Brute Force technique.

Figure 13 shows the result of comparing the irises of the same people (mated-comparison) with the calculated similarity coefficient. On the other hand, Figure 14 shows the result of comparing the irises of different people (non-mated comparison). Figures show the key points detected. All images from each of the IIT Delhi Iris Database (Version 1.0) [31], MMU.v2 database [32], UBIRIS v1 [33], UBIRIS v2 [34], databases were selected for the experiments.

To evaluate the performance of the proposed system, the recognition (accuracy)

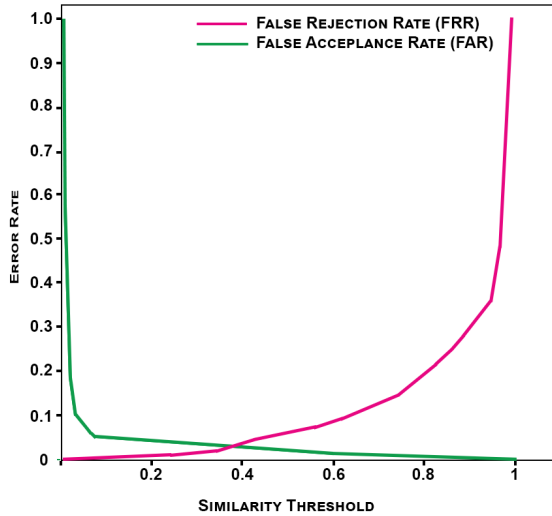


Fig. 12. Diagram illustrating an experiment to select a P threshold.

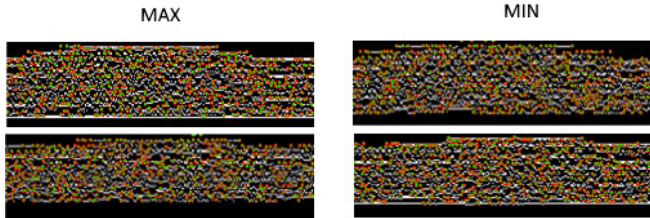


Fig. 13. Comparison of key points for the paths of maximum values ( $P = 0.6072$ ) and minimum values ( $P = 0.731$ ) – mated-comparison.

coefficient was used as an evaluation parameter (11).

$$ACC = (TP + TN) / (TP + TN + FN + FP), \tag{11}$$

where TP – true positive recognition, TN – true negative recognition, FP – false positive recognition, FN – false negative recognition. The above-mentioned AAC parameter ranges from 0, (meaning perfectly correct recognition) to 1, meaning error.

In the second part of our experiment, we used the Siamese Network. The images from each base were divided into a training set and a test set at a ratio of 80% to 20%. The division was applied to each of the classes present in the test sets. In addition, transformations of the source images such as rotation, vertical, and horizontal reflection, zoom and shift along the X or Y axis were used in the testing phase.

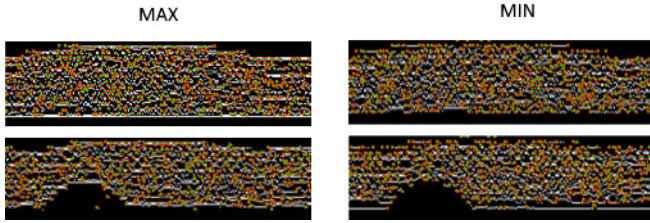


Fig. 14. Comparison of key points for the paths of maximum values ( $P = 0.0273$ ) and minimum values ( $P = 0.0911$ ) – non mated-comparison.

Each class thus contained 15 iris images – 5 images for each input. The Siamese Network uses data augmentation. For this purpose, simple geometric transformations were used – shift, reflection, tilt. The crucial element is the error of validation and training of the network. If the error decreases, the training should continue. If the validation error starts to increase, there is a high probability of over-fitting. It is therefore necessary to set the highest possible number of epochs (e.g., 100 epochs) and, based on the error rates, terminate the training. An epoch is one learning cycle in which the entire training data set is visible. A large number of epochs can result in improved precision up to a certain limit, beyond which the model becomes over-fitted to the data. A small number of epochs, on the other hand, can result in an inappropriate fit to the data. We observed that above 40 epochs, the model does not improve.

The value of  $m$  in Eq. (10) must be chosen experimentally and depends on the domain of application. The value of  $m = 1$  was experimentally determined. In Table 1, we have presented the results of experiments to determine the optimal  $m$  parameter.

The neural network must have correctly prepared data. One of the most important rules is that the input data must have the same size.

In our neural network proposal, we used a  $4 \times 1$  kernel with 6 to 64 filters. Small kernels can extract much more information from the input data containing highly local functions. The smaller kernel size also leads to a smaller reduction in the dimensions of the layers, allowing for deeper architecture. Other parameters of our network – max pooling with a pool size of 2 and stride 2 and utilize dropout of value 0.23 between the pooling and convolutional layers. The dropout method is very efficient, because in every pass the connections are randomly turned off. This ensures that the neural

Tab. 1. Values of parameter  $m$  with corresponding accuracy of Siamese Network.

$m$	0.5	0.75	1	1.25	1.5
<b>Accuracy of the Siamese Network (%)</b>	88	92	97	95	89

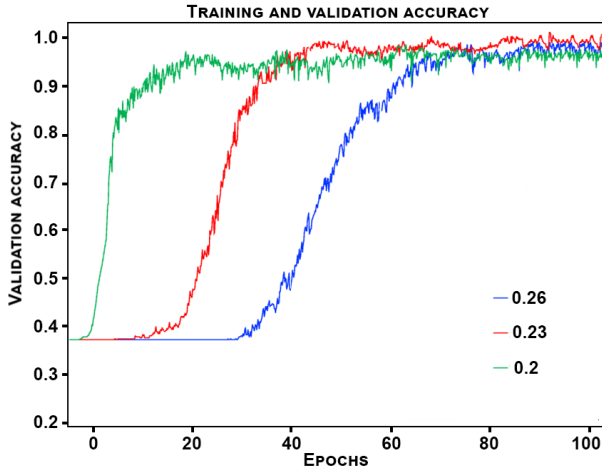


Fig. 15. Experiment results for different values of the dropout parameter.

network does not learn “by heart” too quickly, because the architecture changes a little bit every recalculation by resetting the random connections of the neurons. During the experiments, we tested the parameter dropout in ranges of 0.20 to 0.26, with a step of 0.03. The results of these experiments can be seen in Figure 15.

Table 2 presents the results of measuring the execution time of individual stages of the algorithm we developed. Table 3 presents a comparison of the proposed method to the three methods described at the beginning of this article. To measure execution time, we used BenchmarkDotNet [45]. The test platform was a computer equipped i7-11700K CPU (central processing unit) with NVIDIA TITAN RTX GPU (graphics processing unit) was used.

The decision on the quality of the biometric verification method is assessed by the values of the FAR, FRR and EER coefficients. A wrong acceptance may indicate a security hole, while an unfair rejection becomes embarrassing for the legitimate user. The compromise to the above is the EER factor. The ROC (receiver operating characteristic) curve allows us to determine and indicate the efficiency of biometric comparators, maintaining a compromise between the FAR and FRR coefficients.

We divided our experiments into two groups. In the first experimental group, we analysed and compared the performance of our chosen algorithms for images recorded in the IIT Delhi Iris Database (Version 1.0) [31], MMU.v2 database [32], UBIRIS v1 [33]. These are collections of images recorded in a limited environment. On the other hand, in the second experimental group, we used UBIRIS v1 database [33] comparing the effectiveness of the algorithm with UniNet [3], DRFNet [5] and GraphNet [6]. The

results of the first phase of our experiments are presented below. The authors repeated the experiments 30 times, and the reported results are the arithmetic means.

FRR is the ratio of the false negatives to the sum of the true positive and false negative. The test allowed the FRR ratio at the level of 1.80% (Brute Force) and 0.70% (Siamese Network) to be determined. The FAR coefficient for the implemented algorithm was determined at the level of 2.80% (Brute Force) and 2.10% (Siamese Network). FAR is the ratio of the false positive to the sum of the false positive and true negative.

In contrast, Table 4 shows a comparison of the accuracy of the proposed method for each database. A similar comparison for each of the tested bases for other methods is presented in Table 5.

The maximum execution time of the algorithm is just over two seconds (2229.10 ms, 2178.30 ms), the shortest time was less than a second (125.50 ms, 178.30 ms). This made it possible to obtain an average time of one second (1077.85 ms, 1015.30 ms) for the Brute Force and Siamese Network methods, respectively.

In the second phase of testing, we used the previously discussed neural networks comparing the results they obtained for images from the UBIRIS v2 database [34].

In a paper by Zao et al. [3] investigated the effectiveness of the UniNet neural network in dissecting the iris of the eye using on images recorded in infrared light – in our test we

Tab. 2. Time complexity of the proposed method.

Algorithm step	Time [ms]		
	Minimum	Maximum	Average
Locating and Segment Iris	104.00	2161.00	1000.00
Normalization	2.00	3.00	2.50
Encoding	8.20	10.30	9.25
Match (Brute Force)	11.30	54.80	66.10
Match (Siamese Network)	3.10	4.00	3.55
<b>Total (Brute Force)</b>	<b>125.50</b>	<b>2229.10</b>	<b>1077.85</b>
<b>Total (Siamese Network)</b>	<b>117.30</b>	<b>2178.30</b>	<b>1015.30</b>

Tab. 3. Time complexity, accuracy, EER of the proposed method with other known algorithms (average value) – IIT Delhi Iris Database (Version 1.0) [31], MMU.v2 database [32], UBIRIS v1 [33].

Algorithm	Time (s)	Accuracy (%)	EER (%)
Wang et al. [22]	1.13700	95.30	0.60
Yao et al. [30]	1.08820	91.00	0.91
Rathgeb et al. [12]	1.14990	86.00	1.17
<b>Proposed method (BF)</b>	<b>1.07785</b>	<b>97.74</b>	<b>0.26</b>
<b>Proposed method (SN)</b>	<b>1.01530</b>	<b>98.70</b>	<b>0.17</b>

used the UBIRIS v2 database [34]. For iris recognition, UniNet can use various image processing techniques such as edge detection, segmentation and normalization of iris images. The network can also take into account different lighting conditions and iris positions to ensure recognition performance.

Tab. 4. Comparison of accuracy, EER, FAR, FRR of the proposed method for each used database.

Database	Accuracy (%)	EER (%)	FAR (%)	FRR (%)
Brute Force				
MMU.v2 database [32]	97.31	0.34	2.60	2.90
IIT Delhi Iris Database (Version 1.0) [31]	98.70	0.19	2.40	0.60
UBIRIS v1 [33]	97.20	0.26	3.40	1.80
Siamese Network				
MMU.v2 database [32]	98.60	0.20	2.40	1.30
IIT Delhi Iris Database (Version 1.0) [31]	99.20	0.13	1.30	0.30
UBIRIS v1 [33]	98.20	0.20	2.50	0.60

Tab. 5. Comparison of accuracy and EER of Wang et al. [22], Yao et al. [30], Rathgeb et al. [11] method for each used database (average value).

Database	Accuracy (%)	EER (%)	FAR (%)	FRR (%)
Wang et al. [22]				
MMU.v2 database [32]	95.10	0.20	2.40	0.50
IIT Delhi Iris Database (Version 1.0) [31]	97.80	0.23	2.20	0.64
UBIRIS v1 [33]	93.00	0.17	2.80	1.40
Yao et al. [30]				
MMU.v2 database [32]	86.50	1.70	2.60	2.10
IIT Delhi Iris Database (Version 1.0) [31]	98.50	0.12	1.80	0.30
UBIRIS v1 [33]	88.00	0.91	2.30	1.50
Rathgeb et al. [12]				
MMU.v2 database [32]	88.20	0.71	1.60	1.10
IIT Delhi Iris Database (Version 1.0) [31]	91.60	0.67	0.90	1.00
UBIRIS v1 [33]	78.20	2.13	1.70	3.10

DRFNet [5] is another neural network model used for iris recognition. This network consists of several blocks with convolution layers, ReLU (Rectified Linear Unit), Batch Normalization, Pooling layers and Global Average Pooling. The entire network is also based on recursive layer pooling.

The latest GraphNet neural network model for iris recognition [6] is based on a graph-based data structure. It consists of two main blocks: a feature extraction block and a classification block. The feature extraction block uses convolutional neural networks to extract important iris features. The classification block uses graph data structure for accurate classification.

In Table 6 we have presented a comparison of the proposed method to the methods presented above for the UBIRIS v2 database [34]. The tests were performed using pre-trained neural networks.

Figures 16-17 show the relation between FPR as the False Positive Rate against the TPR as the True Positive Rate (12).

$$TPR = TP/(TP + FN), \quad FPR = FP/(TN + FP) \quad (12)$$

Images in which the iris was more obscured by eyelids or eyelashes gave the algorithm [12] more problems. The algorithm [12] was able to correctly extract the correct points needed to create paths with extreme values. Our proposed modification is resistant to the above-mentioned problems. Examples of these images are shown in Figure 18. Our CNN model reaches almost 100% accuracy and as one can see the network training should finish at the 40th epoch (Fig. 19, Fig. 20); increasing the training period does not significantly affect the network quality. Fig. 20 shows the training curves for all three networks, which are part of our Siamese Network.

## 5. Discussion

The iris extraction algorithm proposed by [12] is sensitive to light reflections occurring near the centre of the pupil which causes inaccurate segmentation of the iris. In addition,

Tab. 6. Time complexity, accuracy of the proposed method with other known algorithms UniNet [3], DRFNet [5], GraphNet [6] – UBIRIS v2 [33].

Algorithm	Time (ms)	Accuracy (%)	EER (%)
UniNet [3]	6.10	99.32	0.08
DRFNet [5]	5.80	99.36	0.06
GraphNet [6]	6.70	99.24	0.11
<b>Proposed method (SN)</b>	<b>5.90</b>	<b>99.15</b>	<b>0.18</b>

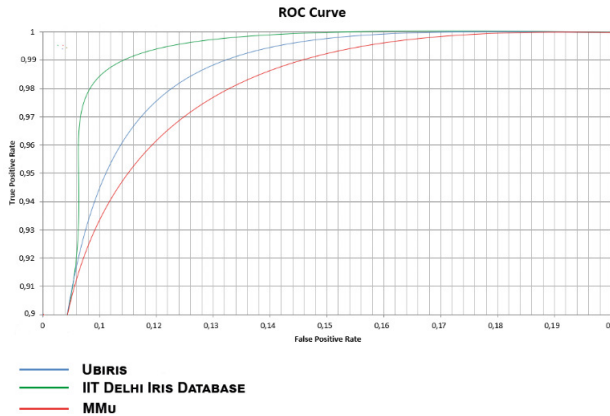


Fig. 16. ROC curve (Brute Force) – UBIRIS v1 [33], MMU.v2 database [32], IIT Delhi Iris Database (Version 1.0) [31].

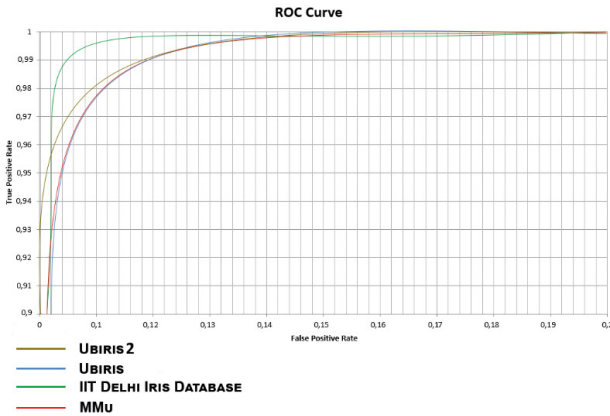


Fig. 17. ROC curve (Siamese Network) – UBIRIS v2 [34], UBIRIS v1 [33], MMU.v2 database [32], IIT Delhi Iris Database (Version 1.0) [31].

the path extraction method does not eliminate all extreme values, which causes large inaccuracies when comparing iris patterns. The elimination of noisy areas in the paper [12] is based on the elimination of the area where noise, due to eyelashes and eyelids, is most likely to occur, without considering noise in other areas of the iris. The extracted iris areas are subjected to the Gaussian blur algorithm, which also does not guarantee getting rid of extreme values from the extracted area. The experiments prove that, in the case of analysing the paths of extremes of grey point values, it is enough to analyse the



Fig. 18. Example of images which are discarded in our experimentations for our segmentation method – (a) UBIRIS v1 [33], (b) IIT Delhi Iris Database (Version 1.0) [31].

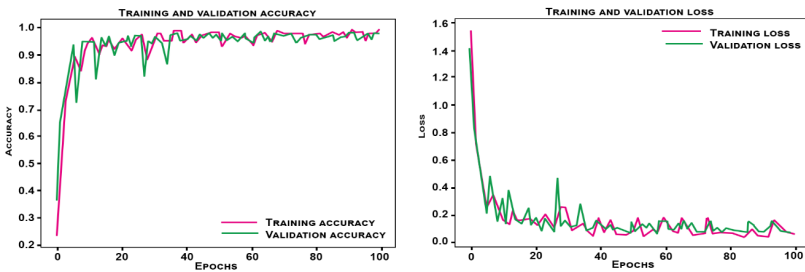


Fig. 19. Accuracy and loss curves for all databases.

appropriately extracted points together with their descriptors. This procedure reduces the amount of data required for analysis.

In the second method we reproduced [30], feature extraction was performed using the Haar wavelet transform, and classification was done by clustering the wavelet feature data using the K-means method. Local iris texture features were extracted using a Log-Gabor filter. The method produced similar results in all tested databases and proved inferior to the proposed method.

In both algorithms [30] and [12], a small fragment of the iris area is analysed, which distinguishes the two approaches from the one proposed here and appears to be an inferior approach to solving the iris recognition problem.

The proposal to eliminate areas obscured by eyelids and eyelashes using rigidly chosen parameters [30] [12] is less effective for highly noisy images. The experiments we conducted prove that using the entire iris area gives better results [22].

The EER was also studied, as it is a compromise between the convenience and effectiveness of the biometric recognition system. The EER measure is determined using the FRR and FAR ratios discussed above. A system with a lower EER is more accurate. The EER value indicates that the proportion of false acceptances is equal to the proportion of false rejections. The average value of the EER 0.26 (Brute Force) coefficient achieved

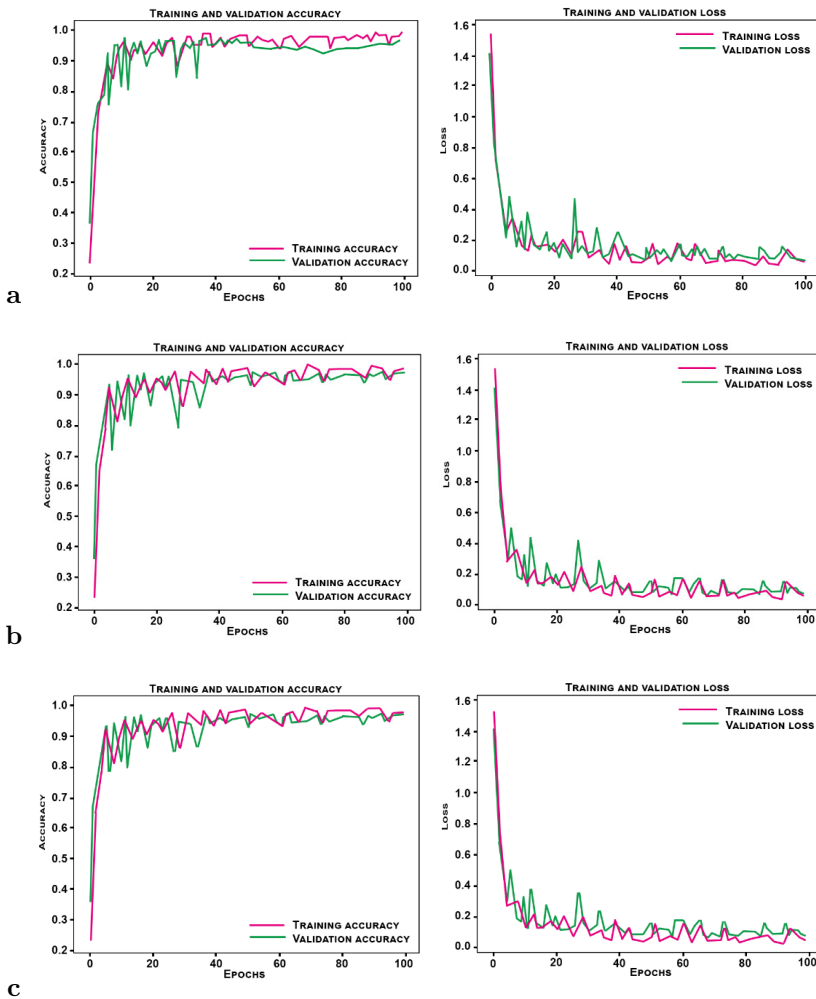


Fig. 20. Accuracy and loss curves – (a) anchor, (b) positive, (c) negative.

by us is comparable to other methods described in the introduction. If we look at the individual iris databases in more detail, it can be noticed that in the case of IIT Delhi Iris Database (Version 1.0) [31], we managed to achieve an EER value of 0.24. This is the best result of all the previously discussed works.

However, the obtained mean accuracy value of proposed method (Brute Force), equal

to 97.74% and a variant of proposed method using the Siamese Network achieved efficiency of 98.70% with an EER of 0.17. The Siamese Network proved to be almost 20 times faster than the Brute Force.

Overall, the IIT Delhi Iris Database (Version 1.0) [31] shows the best results. This is mainly because the IIT Delhi Iris Database (Version 1.0) [31] presents well-contrasted images with appropriate resolution for feature extraction methods based on key points, although this database is strongly disrupted by eyelid and lash occlusions. The MMU.v2 database [32] has a lower image resolution. The UBIRIS v1 [33] database is noisier in terms of lighting, motion blur, tilt angle and viewing direction. We therefore can claim that the proposed method is the most stable and has the highest performance in the three databases considered. Moreover, by comparing the results with those presented in Tables 2, 3, 4 one can see the benefits of using our suggested modification of the algorithm in [12] and indicates the superiority of image analysis methods using CNNs over methods using traditional image processing. The proposed method is better than the methods proposed by Wang et al. [22], Yao et al. [30], Rathgeb et al. [12].

The UBIRIS v2 database [34] is one of the largest and most diverse databases of irises from different individuals. This diversity allows testing the performance of iris recognition under different conditions, such as varying lighting, different cameras, and different iris positions. In addition, it is one of the most popular and widely used iris databases for testing recognition algorithms. Tests on the UBIRIS v2 database [34] have shown the great potential of proposed algorithm. Compared to other neural networks, the result obtained is minimally inferior. The improvement over previously tested databases may be due to a different approach to the iris segmentation problem. On the other hand, a better algorithm execution time was obtained from UniNet [3] and GraphNet [6] algorithms. The execution time of proposed algorithm was 5.90 ms, which was only 0.10 ms worse than that of the DRFNet algorithm [5]. The EER parameter of 0.18 achieved in the test demonstrates the high quality of proposed algorithm.

## 6. Conclusions

The use of the method of recognizing the iris of the eye with the use of encoding with extreme values of shades of grey and the use of the Harris-Laplace algorithm [40] and SIFT keypoint descriptor [41] Siamese Network [43] gave promising results. The achieved EER, FRR and FAR coefficients allow us to conclude that the proposed method retained a compromise between the efficiency and the speed of comparison of patterns. Through our verification process, we have determined that the utilization of Siamese neural networks in combination with SIFT descriptors serves as a viable alternative to other existing methods, as described in the literature, which rely on point descriptors and neural networks for iris recognition.

Our research shows that the introduction of simple components to methods developed

by other authors [12] allows to significantly improve the quality of these algorithms, providing modern results in the field of iris biometrics. We provide conclusive evidence that valuable information pertaining to the structure and characteristics of the iris can indeed be successfully extracted from the paths of extreme values for different shades of grey. This approach can be considered as an extension of the previously described iris recognition methods, with the added benefit of significantly enhancing their efficiency and effectiveness.

Unfortunately, the method turned out to be less effective in the case of images recorded in visible light and heavily noisy. The method achieves the best results with well-contrasted images. Proposed algorithm can be implemented on more bases. Experiments have proved the effectiveness of the method on images captured in visible light and on images captured in infrared light (weakly and strongly contrasted). The algorithm is unable to properly extract paths if there are large areas with similar values. In this case, the paths overlap, causing distortions in the final stage of extracting these paths.

Future work will focus on the use of artificial intelligence to dynamically determine the degree of similarity and to extract high and low value paths, from noisy images in particular. The described method is applicable in the conditions of the tested image databases. Subsequent studies will focus on the possibilities of applying the method in different environments and image capturing conditions. In addition, the authors intend to eliminate the drawbacks of the developed method, so that it is effective for iris images captured with, for example, smartphones [47] with account eye iris rotation (use more challenging databases). Images captured with an SLR (Single-Lens Reflex) camera that is several years old [32] are characterized by minimal chromatic aberrations and provide sharp, crisp images even from a very short distance compared to even the latest smartphones [46]. Images captured with a DSLR (Digital Single-Lens Reflex) camera are usually deliberately underexposed, lacking saturation and digital overexposure, so that later in further processing we can adequately stretch the tonal space and enhance what we care most about, highlighting in this case the subtle differences between iris points. Images of the iris, taken in infrared light, have additional information about the iris pattern. In the work of Hosseini, et al. [47], an extensive comparison was made between the visible-light and infrared iris registration methods.

## References

- [1] Willoughby, C. E., Ponzin, D., Ferrari, S., Lobo, A., Landau, K., Omid, Y. (2010). Anatomy and physiology of the human eye: effects of mucopolysaccharidoses disease on structure and function – A review. *Clinical & Experimental Ophthalmology*, 38:2–11. doi:10.1111/j.1442-9071.2010.02363.x
- [2] Das, P., Holsopple, L., Rissacher, D., Schuckers, M., Schuckers, S. (2021). Iris Recognition Performance in Children: A Longitudinal Study. *IEEE Transactions on Biometrics, Behavior, and Identity Science*, 3(1):138–151. doi:10.1109/TBIOM.2021.3050094
- [3] Zhao, Z., Kumar, A. (2017). Towards more accurate iris recognition using deeply learned spatially

- corresponding features. In *Proceedings of the IEEE International Conference on Computer Vision (ICCV)*, pp. 3809–3818. doi:10.1109/ICCV.2017.411
- [4] Hajari, K., Gawande, U., Golhar, Y. (2016). Neural network approach to iris recognition in noisy environment. *Procedia Computer Science*, 78:675–682. doi:10.1016/j.procs.2016.02.116
- [5] Wang, K., Kumar, A. (2019). Toward more accurate iris recognition using dilated residual features. *IEEE Transactions on Information Forensics and Security*, 14(12):3233–3245. doi:10.1109/TIFS.2019.2913234
- [6] Ren, M., Wang, Y., Sun, Z., Tan, T. (2020, April). Dynamic graph representation for occlusion handling in biometrics. In *Proceedings of the AAAI Conference on Artificial Intelligence*, Vol. 34, No. 07, pp. 11940–11947. doi:10.1609/aaai.v34i07.6869
- [7] Chicco, D. (2021). Siamese Neural Networks: An Overview. In: Cartwright, H. (eds). *Artificial Neural Networks. Methods in Molecular Biology*, Vol. 2190. Humana, New York, NY. [https://doi.org/10.1007/978-1-0716-0826-5\\_3](https://doi.org/10.1007/978-1-0716-0826-5_3)
- [8] Rathgeb, C., Wagner, J., Busch, C. (2019). SIFT-based iris recognition revisited: prerequisites, advantages and improvements. *Pattern Analysis and Applications*, 22:889–906. doi:10.1007/s10044-018-0719-y
- [9] Tareen, S. A. K., Raza, R. H. (2023, March). Potential of SIFT, SURF, KAZE, AKAZE, ORB, BRISK, AGAST, and 7 More Algorithms for Matching Extremely Variant Image Pairs. In *Proceedings of the 2023 4th International Conference on Computing, Mathematics and Engineering Technologies (iCoMET)*, pp. 1–6. IEEE. doi:10.1109/iCoMET57998.2023.10099250
- [10] Zhao, Y., Zhai, Y., Dubois, E., Wang, S. (2016). Image matching algorithm based on SIFT using color and exposure information. *Journal of Systems Engineering and Electronics*, 27(3), 691–699. doi:10.1109/JSEE.2016.00072
- [11] Liu, C., Xu, J., Wang, F. (2021). A review of keypoints' detection and feature description in image registration. *Scientific Programming*, 1–25, 2021. doi:10.1155/2021/8509164
- [12] Rathgeb, C., Uhl, A. (2010, June). Secure iris recognition based on local intensity variations. In *Proceedings of the International Conference Image Analysis and Recognition (ICIAR)*, pp. 266–275. Springer, Berlin, Heidelberg. doi:10.1007/978-3-642-13775-4\_27
- [13] Lee, M. B., Kang, J. K., Yoon, H. S., Park, K. R. (2021). Enhanced iris recognition method by generative adversarial network-based image reconstruction. *IEEE Access*, 9:10120–10135. doi:10.1109/ACCESS.2021.3050788
- [14] Yang, K., Xu, Z., Fei, J. (2021). Dualsanet: Dual spatial attention network for iris recognition. In *Proceedings of the IEEE/CVF Winter Conference on Applications of Computer Vision*, pp. 889–897. doi:10.1109/WACV48630.2021.00093
- [15] Chen, Y., Zeng, Z., Gan, H., Zeng, Y., Wu, W. (2021). Non-segmentation frameworks for accurate and robust iris recognition. *Journal of Electronic Imaging*, 30(3):033002. doi:10.1117/1.JEI.30.3.033002
- [16] Winston, J. J., Hemanth, D. J., Angelopoulou, A., Kapetanios, E. (2021). Hybrid deep convolutional neural models for iris image recognition. *Multimedia Tools and Applications*, 81(7):9481–9503. doi:10.1007/s11042-021-11482-y
- [17] Liu, M., Zhou, Z., Shang, P., Xu, D. (2019). Fuzzified image enhancement for deep learning in iris recognition. *IEEE Transactions on Fuzzy Systems*, 28(1):92–99. doi:10.1109/TFUZZ.2019.2912576
- [18] Chen, Y., Wu, C., Wang, Y. (2020). T-center: A novel feature extraction approach towards large-scale iris recognition. *IEEE Access*, 8:32365–32375. doi:10.1109/ACCESS.2020.2973433

- [19] Liu, G., Zhou, W., Tian, L., Liu, W., Liu, Y., Xu, H. (2021). An efficient and accurate iris recognition algorithm based on a novel condensed 2-ch deep convolutional neural network. *Sensors*, 21(11):3721. doi:10.3390/s21113721
- [20] Ahmadi, N., Akbarizadeh, G. (2018). Hybrid robust iris recognition approach using iris image pre-processing, two-dimensional gabor features and multi-layer perceptron neural network/PSO. *IET Biometrics*, 7(2):153–162. doi:10.1049/iet-bmt.2017.0041
- [21] Ahmadi, N., Nilashi, M., Samad, S., Rashid, T. A., Ahmadi, H. (2019). An intelligent method for iris recognition using supervised machine learning techniques. *Optics & Laser Technology*, 120:105701. doi:10.1016/j.optlastec.2019.105701
- [22] Wang, Y., Zheng, H. (2021, February). An improved Iris recognition method based on wavelet packet transform. *Journal of Physics: Conference Series*, Vol. 1744, No. 4, p. 042239. IOP Publishing. doi:10.1088/1742-6596/1744/4/042239
- [23] Bala, N., Vyas, R., Gupta, R., Kumar, A. (2021). Iris Recognition Using Improved Xor-Sum Code. In *Proceedings of the Conference on Security and Privacy*, pp. 107–117. Springer, Singapore. doi:10.1007/978-981-33-6781-4\_9
- [24] Galdi, C., Dugelay, J. L. (2017). FIRE: Fast Iris REcognition on mobile phones by combining colour and texture features. *Pattern Recognition Letters*, 91:44–51. doi:10.1016/j.patrec.2017.01.023
- [25] Lv, L., Yuan, Q., Li, Z. (2019). An algorithm of Iris feature-extracting based on 2D Log-Gabor. *Multimedia Tools and Applications*, 78(16):22643–22666. doi:10.1007/s11042-019-7551-2
- [26] Abbasi, M. (2019). Improving identification performance in iris recognition systems through combined feature extraction based on binary genetics. *SN Applied Sciences*, 1(7):1–14. doi:10.1007/s42452-019-0777-9
- [27] Barpanda, S. S., Sa, P. K., Marques, O., Majhi, B., Bakshi, S. (2018). Iris recognition with tunable filter bank based feature. *Multimedia Tools and Applications*, 77(6):7637–7674. doi:10.1007/s11042-017-4668-z
- [28] Barpanda, S. S., Majhi, B., Sa, P. K., Sangaiah, A. K., Bakshi, S. (2019). Iris feature extraction through wavelet mel-frequency cepstrum coefficients. *Optics & Laser Technology*, 110:13–23. doi:10.1016/j.optlastec.2018.03.002
- [29] Gad, R., Talha, M., Abd El-Latif, A. A., Zorkany, M., Ayman, E. S., Nawal, E. F., Muhammad, G. (2018). Iris recognition using multi-algorithmic approaches for cognitive internet of things (CIoT) framework. *Future Generation Computer Systems*, 89:178–191. doi:10.1016/j.future.2018.06.020
- [30] Liping, Y., Zhongliang, P. (2019). Iris recognition method based on Harr wavelet and Log-Gabor transform [J]. *Application of Electronic Technique*, 45(4):113–117. doi:10.16157/j.issn.0258-7998.183173
- [31] Kumar, A. and Passi, A (2010). Comparison and combination of iris matchers for reliable personal authentication, *Pattern Recognition*, 43(3):1016–1026. doi:10.1016/j.patcog.2009.08.016
- [32] MMU v2 MMU Iris Database, Malaysia Multimedia University, <http://andyzeng.github.io/downloads/MMU2IrisDatabase.zip>. [Dataset, accessed 1 November 2021]
- [33] Proença, H. and Alexandre, L. A., 2005, September. UBIRIS: A noisy iris image database. In *Proceedings of the International Conference on Image Analysis and Processing (ICIAP)*, pp. 970–977. Springer, Berlin, Heidelberg. doi:10.1007/11553595\_119
- [34] [dataset] Proença, H., Filipe, S., Santos, R., Oliveira, J. and Alexandre, L. A. (2010). The UBIRIS.v2: A Database of Visible Wavelength Iris Images Captured On-The-Move and At-A-Distance, *IEEE Transactions on Pattern Analysis and Machine Intelligence*, 12(8):1529–1535. doi:10.1109/TPAMI.2009.66

- [35] Malinowski, K., Saeed, K. (2022). An Efficient Algorithm for Boundary Detection of Noisy or Distorted Eye Pupil. In *Proceedings of the Conference on Advanced Computing and Systems for Security*, Vol. 13, pp. 51–59. Springer, Singapore. doi:10.1007/978-981-16-4287-6\_4
- [36] Malinowski, K., Saeed, K. (2022). An iris segmentation using harmony search algorithm and fast circle fitting with blob detection. *Biocybernetics and Biomedical Engineering*, 42(1):391–403. doi:10.1016/j.bbe.2022.02.010
- [37] Moslhi, O. M. (2020). New full Iris Recognition System and Iris Segmentation Technique Using Image Processing and Deep Convolutional Neural Network. *International Journal of Scientific Research in Multidisciplinary Studies*, 6(3):20–27. [https://www.isroset.org/journal/IJSRMS/full\\_paper\\_view.php?paper\\_id=1775](https://www.isroset.org/journal/IJSRMS/full_paper_view.php?paper_id=1775)
- [38] Malgheet, J. R., Manshor, N. B., Affendey, L. S., Abdul Halin, A. B. (2021). Iris Recognition Development Techniques: A Comprehensive Review. *Complexity*, 2021. doi:10.1155/2021/6641247
- [39] Alvarez-Betancourt, Y., Garcia-Silvente, M. (2016). A keypoints-based feature extraction method for iris recognition under variable image quality conditions. *Knowledge-Based Systems*, 92:169–182. doi:10.1016/j.knosys.2015.10.024
- [40] Tuytelaars, T., Mikolajczyk, K. (2008). *Local invariant feature detectors: A survey*. Now Publishers Inc. doi:10.1561/9781601981394
- [41] Lowe, D. G. (2004). Distinctive image features from scale-invariant keypoints. *International Journal of Computer Vision*, 60(2):91–110. doi:10.1023/B:VISI.0000029664.99615.94
- [42] Noble, F. K. (2016, November). Comparison of OpenCV’s feature detectors and feature matchers. In *Proceedings of the 2016 23rd International Conference on Mechatronics and Machine Vision in Practice (M2VIP)*, pp. 1-6. IEEE. doi:10.1109/M2VIP.2016.7827292
- [43] Chopra, S., Hadsell, R., LeCun, Y. (2005, June). Learning a similarity metric discriminatively, with application to face verification. In *Proceedings of the 2005 IEEE Computer Society Conference on Computer Vision and Pattern Recognition (CVPR’05)*, Vol. 1, pp. 539–546. IEEE. doi:10.1109/CVPR.2005.202
- [44] Schuetzke, J., Benedix, A., Mikut, R., Reischl, M. (2020, November). Siamese Networks for 1D Signal Identification. In *Proceedings of the 30. Workshop on Computational Intelligence*, Berlin, 26-27 November, 2020. Vol. 26, p. 17. KIT Scientific Publishing. doi:10.5445/KSP/1000124139
- [45] .NET Foundation and contributors. BenchmarkDotNet version 0.13.1, Copyright (c) 2013-2021, <https://benchmarkdotnet.org/>
- [46] De Marsico, M., Nappi, M., Riccio, D., Wechsler, H. (2015). Mobile iris challenge evaluation (MICHE)-I, biometric iris dataset and protocols. *Pattern Recognition Letters*, 57:17–23. doi:10.1016/j.patrec.2015.02.009
- [47] Hosseini, M. S., Araabi, B. N., Soltanian-Zadeh, H. (2010). Pigment melanin: Pattern for iris recognition. *IEEE Transactions on Instrumentation and Measurement*, 59(4):792–804. doi:10.1109/TIM.2009.2037996



**Prof. Khalid Saeed** is a full Professor of Computer Science at Bialystok University of Technology and a half-time visiting professor at Universidad de La Costa, Barranquilla, Colombia. He was with Warsaw University of Technology in 2014-2019 and with AGH Krakow in 2008-2014. He received his B.Sc. Degree from Baghdad University in 1976, M.Sc. and Ph.D. (distinguished) Degrees from Wroclaw University of Technology in Poland in 1978 and 1981, respectively. He received his D.Sc. Degree (Habilitation) in Computer Science from the Polish Academy of Sciences in Warsaw in 2007. He was nominated by the President of Poland for the title of Professor in 2014. He has published more than 250 publications including about 120 journal papers and book chapters, about 100 peer reviewed conference papers, edited 50 books, journals and Conference Proceedings, written 13 text and reference books (h-index 19 in WoS and 15 in SCOPUS base). He supervised more than 15 Ph.D. and 150 M.Sc. theses. He gave more than 50 invited lectures and keynotes in different universities in Europe, China, India, South Korea, Serbia, Germany, Japan, and Canada, on biometric image processing and analysis. He received more than 30 academic awards. He is also a member of more than 15 editorial boards of international journals and conferences. He was selected as the IEEE Distinguished Speaker, from 2011 to 2016. He is also the Editor-in-Chief of *International Journal of Biometrics* with Inderscience Publishers.



**Kamil Malinowski** is a Ph.D. student in Computer Science at Bialystok University of Technology. His research focuses on bi-modal biometric systems, where he explores the intersection of computer science and biometrics. With a strong background in both theory and practice, is well-versed in various aspects of biometric data acquisition, image processing, signal processing, biometric feature matching algorithms, performance evaluation of biometric systems, as well as privacy and security concerns related to biometric data. Aside from his academic pursuits, also actively contributes to the field of cybersecurity. He works as a trainer at Altkom Akademia, where he shares his expertise in attack protection, risk management, monitoring, detection, and response to cyber threats. His practical experience in the industry allows him to provide valuable insights and knowledge to trainees, equipping them with the necessary skills to safeguard against cyber threats on a daily basis.